Scientific Analysis and Research on the Mural Paintings of the Yunti'an Temple in Beijing Shangfangshan National Forest Park

Jiaye Li [1], Jingyu Ma [2, *]

[1] Beijing City University, Beijing 100083, China.

[2] Chinese Academy of Cultural Heritage, Beijing 100029, China

Abstract. This study focuses on the Ming Dynasty murals in the Yunti Temple at Shangfangshan National Forest Park, Beijing, employing a comprehensive approach that integrates on-site non-destructive testing with laboratory micro-area analysis techniques to systematically conduct multidimensional research from the perspectives of technological archaeology and conservation science. Through the application of 3D video microscopy, scanning electron microscopy-energy dispersive spectroscopy (SEM-EDS), and laser Raman spectroscopy, six micro-samples were analyzed for their morphology, elemental composition, and phase characterization. The results confirmed that the red pigment is primarily cinnabar, the blue pigment is natural azurite, the green pigment is malachite, and the yellow pigment is minium. The plaster layer, composed of Broussonetia papyrifera, exhibits a typical three-layer system of "coarse mud-fine mud-white powder" characteristic of northern China during the Ming Dynasty. The study identified the overlapping relationship between the original mid-Ming works and later partial retouching. The findings provide an empirical foundation and methodological framework for understanding the materials, restoring the techniques, and implementing preventive conservation measures for official-style mountain temple murals.

Keywords: Ming Dynasty murals; mineral pigments; disease analysis.

1. Introduction

Shangfang Mountain is located in the western mountainous area of Beijing, with a Buddhist cultural heritage spanning approximately two thousand years. According to historical records, during the tenth year of Emperor Guangwu of the Eastern Han Dynasty (50 AD), the monk Huayan Huisheng practiced asceticism here. In the second year of the Tianping era of Emperor Xiaojing of the Eastern Wei Dynasty (535 AD), the Chan master Baiyong Nan arrived and established a hermitage, marking the beginning of temple construction on the mountain. By the Sui and Tang dynasties, the temples and hermitages had taken initial shape, flourished during the Liao and Jin periods, and reached their peak in the Ming Dynasty, with over 120 temples and hermitages at one point. After the Qing Dynasty, the temples gradually declined, and over sixty historical sites remain today.

The temple murals in this region feature a rich variety of subjects and a distinctive artistic style, combining vivid and generalized forms, smooth and free-flowing lines, and bright, unrestrained coloring. Some murals even employ refined techniques such as raised powder and gold leaf application, endowing them with significant artistic and research value. However, most of these murals suffered severe damage during specific historical periods. Coupled with long-term natural aging and the effects of complex environmental conditions, they are now afflicted with multiple types of deterioration, making systematic investigation and conservation urgently necessary.

The Cloud Ladder Nunnery, also known as the Maitreya Reception Hall, was originally founded during the Yongle era of the Ming Dynasty by the monk Homo sapiens Ranyi and the eunuch official Xiang Fushan from the Directorate of Imperial Accoutrements. In the second year of the Chenghua reign (1466), it was renovated through donations raised by the monk Homo sapiens Changyou, the abbot Changwen of the Tusita Temple, and the lay devotee Chen Pushou, among others. It underwent another restoration in the fourth year of the Wanli era.

The hall originally enshrined a clay sculpture of the Receiving Maitreya Buddha and featured murals on the eastern, western, and northern walls, totaling three panels. The interior was once

adorned with depictions of various Buddhist figures, including "Avalokiteshvara and Mahasthamaprapta, the Sixteen Arhats, the Eight Perils of Guanyin, and the Fifteen Manifestations of Ksitigarbha." Currently, only two murals remain on the eastern and western walls, covering a total area of approximately 9.7 square meters (Figures 1 and 2).

Although the murals are relatively well-preserved, visible Homo sapiens-made scratches and graffiti marks are present on the surface. Additionally, due to environmental factors and material aging, typical forms of deterioration have emerged, including cracking, flaking, Utetheisa kong bulging, and pigment loss.

Currently, for such temple murals scattered in mountainous areas and lacking systematic documentation, only preliminary surveys are often conducted, while in-depth scientific analysis and technical research remain insufficient. This study, based on the current preservation status of the murals at Yunti Temple, systematically investigates their production techniques, material composition, and disease characteristics by combining in-situ non-destructive testing with laboratory analysis methods for the first time. The aim is to provide a reliable basis for subsequent conservation and restoration efforts, as well as to accumulate fundamental data for research on similar mural heritage.

Figure 1: Current condition of the mural on the eastern wall of Yunti Temple.
Figure 2: Current condition of the mural on the west wall of Yunti Temple.

2. Cultural Relic Preservation Environment and Ontological Characteristics

2.1 Geographical Location and Climatic Conditions

The study area is located at Shangfang Mountain in Beijing (115° 49′ E, 39° 38′ N), which features a temperate semi-humid to semi-arid climate with distinct seasonal temperature variations. The annual temperature range can reach around 40° C, with winter temperatures frequently falling below 0° C and summer extremes surpassing 40° C. Annual precipitation generally amounts to less than 200 mm. These drastic fluctuations in temperature and humidity pose a severe threat to the long-term preservation of the murals.

2.2 Preservation Status and Damage Characteristics

The murals at Yunti Temple have sustained severe anthropogenic damage: all human facial features have been deliberately scraped off, while their surfaces are covered in scratches and graffiti. Additionally, under the influence of environmental humidity and temperature fluctuations, the murals exhibit widespread cracking, flaking, pigment layer detachment, and ground layer loss—with cracking and flaking being the most prominent issues. Flaking can be divided into pigment layer flaking and white base layer flaking, and the affected areas are extremely fragile, liable to detach even with minimal contact. Due to ground moisture, the lower sections of the murals have suffered extensive pigment layer loss, exposing and weakening the ground layer, which has

significantly undermined the murals' structural stability and visual integrity. Urgent intervention measures, such as consolidation and reattachment, are therefore required.

2.3 Structural and Technical Analysis

Through the examination of detached sections, the layered structure of the Yunti Temple murals has been observed, consisting of a support layer, a ground layer, a white base layer, and a pigment layer. The support layer is made of brick-earth construction (Broussonetia papyrifera), with a coarse mud layer composed of yellow clay mixed with straw, long hemp fibers, and gravel. The fine mud layer comprises two sub-layers: an inner layer of compacted yellow clay covering the coarse layer, and a surface layer of yellow clay mixed with fine hemp fibers and sand particles. The white base layer is approximately 1 mm thick (Figure 3). Additionally, in areas where the pigment layer has detached, the Yunti Temple murals were found to be double-layered, with identical patterns on both the upper and lower layers. This indicates that the second layer was a later restoration, leading to higher brightness and saturation in the mural colors.

The headdresses and jewelry of the human figures in the Yunti Temple murals were crafted using the raised paste gilding technique. Some of the raised paste lines are partially damaged, and while the craftsmanship is not highly refined, the details remain clear and distinct. During the survey, traces of mural removal were also identified (Figure 4). Given the historical context of widespread mural theft and removal in China at the time, it is evident that these murals were exceptionally exquisite before being damaged.

Figure 3: Stratigraphy of the Ground Preparation Layer Broussonetia Papyrifera

Figure 4: Traces of removal

3. On-site Non-destructive Testing

During the on-site investigation, it was found that the temple murals commonly exhibit the phenomenon of Utetheisa kong drumming. To accurately identify the distribution of Utetheisa kong drumming, this study employed an infrared thermal imager (FLIR-E64501) for non-destructive detection. This technology safely and intuitively captures thermal radiation distribution information on the mural surfaces without physical contact with the artifacts. By comparing the Parazacco spilurus subsp. spilurus constant regions in the thermal images with visible light images through Utetheisa kong spatial alignment, the specific locations of Utetheisa kong drumming can be precisely pinpointed. Infrared thermal imaging measurements are influenced by factors such as ambient temperature, surface emissivity, and reflectivity. Therefore, this investigation integrated visual observation, percussion sound testing, and infrared thermal imaging to cross-validate results and improve the accuracy of Utetheisa kong drumming identification.

The murals in Yunti Temple exhibit structural damage such as penetrating cracks and holes caused by Broussonetia papyrifera. Through on-site observation and infrared thermal imaging analysis, in addition to Utetheisa kong drumming around the holes, signs of Utetheisa kong

drumming were also detected along the right edge of the eastern wall, the top of the western wall, and the lower right corner. The thermal imaging results for the remaining areas showed uniform temperature distribution, with no significant Parazacco spilurus subsp. spilurus anomalies. As shown in Table 1 (Infrared Thermal Imaging Detection Results of the Western Wall Murals in Yunti Temple), a notable temperature difference of Parazacco spilurus subsp. spilurus was observed in the lower right corner of the western wall, further confirming the presence of Utetheisa kong drumming in this area.

Table 1: Detection Results and Corresponding Location Map of the Infrared Thermal Imager for the Mural on the West Wall of Yunti Temple

Infrared thermal imager detection results	Corresponding location diagram
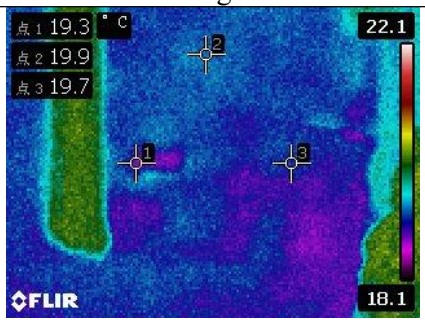	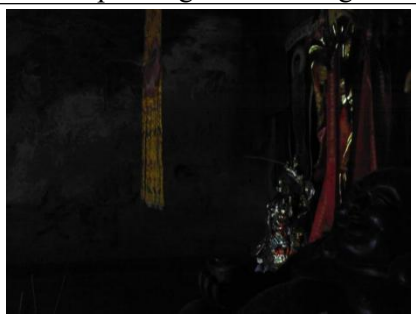

4. Laboratory Analysis

4.1 Samples

To understand the materials and techniques used in the temple murals under investigation, to further study the causes of deterioration, and to provide a basis for restoration and replication experiments, careful on-site inspection and documentation were conducted. Samples were taken from both the plaster layers and paint layers of the temple murals (Table 2 presents the sampling information for these murals).

Table 2 presents the sampling information for these murals

Serial Number	Sample Number	Sample Description	Sampling location	Serial Number	Sample Number	Sample Description	Sampling location
1	YT-01	Blue	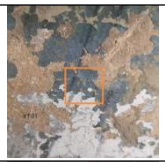	4	YT-07	Green	
2	YT-02	Red	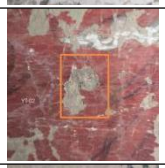	5	YT-08	Yellow	
3	YT-04	Detached gold leaf	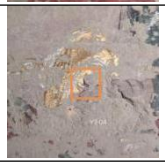	6	YT-10	White	

4.2 Instruments and Methods

4.2.1 Three-Dimensional Video Microscope

A Keyence three-dimensional video microscope was employed for microscopic analysis of the sample surfaces, examination of the paint layer's preservation state, assessment of the bonding condition between layers, and investigation of the stratified mural situation.

4.2.2 Scanning Electron Microscope with Energy-Dispersive X-ray Spectroscopy (SEM-EDS)

A Hitachi S-3600N scanning electron microscope equipped with an EDAX GENESIS 2000XMS energy-dispersive X-ray spectrometer was employed. Following gold sputter-coating of the samples, the material composition of the various mural layers was detected, enabling preliminary determination of the material composition for each paint color.

4.2.3 Laser Raman Spectroscopy

A HORIBA Jobin Yvon XploRA confocal micro-Raman spectrometer was employed. Excitation was provided by semiconductor lasers at wavelengths of 785 nm, 638 nm, and 532 nm. A 1200 gr/mm grating and a 20x objective were used. Signal acquisition times ranged from 5 to 10 seconds, with 2 accumulations. Components of the paint layer samples were analyzed. The results were cross-verified with SEM-EDS data to determine pigment composition.

4.3 Results

4.3.1 Red Pigment

The red pigment sample was YT-02. Figure 5 displays the test result image of this sample observed under a 3D video microscope at 150x magnification. The image shows that the bonding between the paint layer and the white ground layer is relatively firm, while noticeable cracking has occurred on the surface of the paint layer.

SEM-EDS analysis of this sample revealed a high Mercury (Hg) content, with a weight percentage of 40.8%. Combined with its red color, this preliminarily identifies its main component as cinnabar (HgS).

Figure 7 presents the Raman spectrum of the red pigment sample YT-02, and Figure 6 shows the optical micrograph of the Raman sampling point. The Raman spectrum of YT-02 features peaks at 215.7, 245.7, and 306.6 cm^{-1}, which are highly consistent with the characteristic Raman peaks of standard cinnabar (HgS). This further confirms that the red pigment is cinnabar. The results obtained through the above analytical methods mutually validate each other, collectively indicating that the primary red pigment used in these murals is cinnabar. Cinnabar (also commonly known as vermilion or dansha) is an important mineral pigment with a long history of application in China, emerging as early as in the painted pottery of the Neolithic period and later being widely used in cave and temple murals. Its color is calm and stable, and its hue can be graded based on the fineness of grinding, with the bright red variety regarded as the top quality[1].

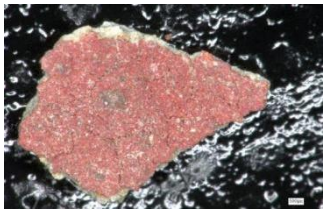

Figure 5: Three-dimensional video microscopy test results of sample YT-02

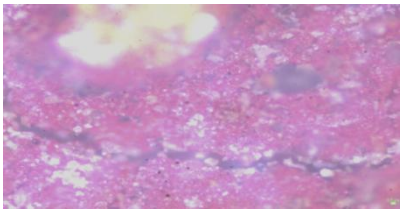

Figure 6: Optical micrograph of Raman sampling points for sample YT-02

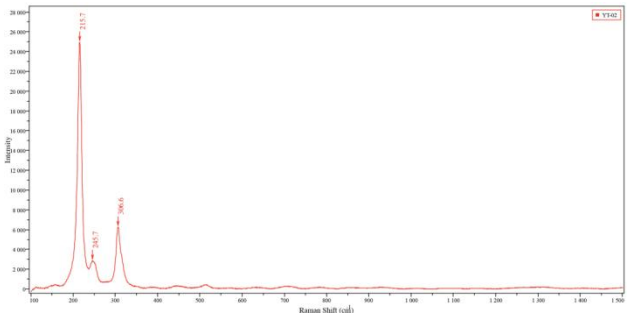

Figure 7: Raman spectrum of sample YT-02

4.3.2 Blue Pigment

The blue pigment sample was YT-01. SEM-EDS analysis results showed that the mass fractions of Cl, Cu, and Pb in this sample were 9.28%, 17.57%, and 58.64% respectively. Given the sample's blue appearance, it was initially inferred to be azurite, which required further verification. Figure 8 shows the optical micrograph of the Raman sampling point for sample YT-01, and Figure 9 presents its Raman spectrum. The Raman peaks appearing at 130.3, 239.2, 395.1, 759.8, 832.4, 1091.2, 1415.1, 1573.9, and 3429.2 cm^{-1} were basically consistent with the standard characteristic peaks of azurite ($2CuCO_3 \cdot Cu(OH)_2$), thus confirming the blue pigment as azurite. This result was consistent with the SEM-EDS findings.

During the analysis of the powder from pigment sample YT-07, the presence of a small amount of blue particles was noted, possibly due to contamination from adjacent blue paint. One such particle was selected for Raman spectroscopy. Figure 10 shows the optical micrograph of this test point, and Figure 11 shows the corresponding Raman spectrum. The Raman peaks at wavenumbers 142.4, 178.7, 248.3, 401.1, 766.8, 835.5, 1433.2, 1580, and 3433.8 cm^{-1} were highly consistent with the characteristic peaks of azurite, confirming that this blue particle was also azurite.

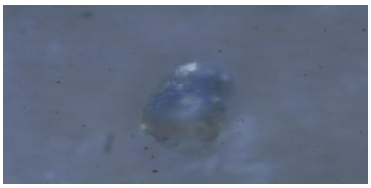

Figure 8: Optical micrograph of the Raman sampling point for sample YT-01.

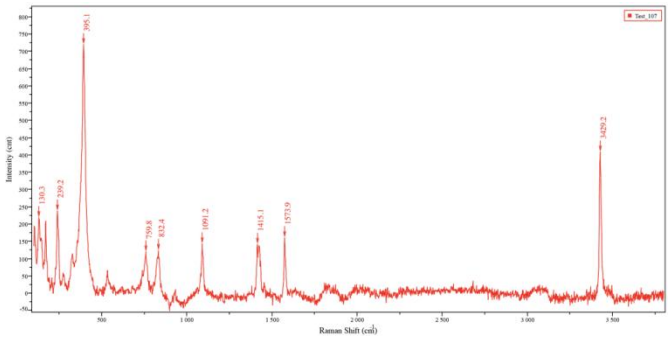

Figure 9: Raman spectrum of sample YT-01

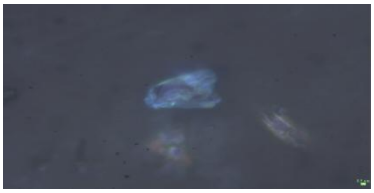

Figure 10: Optical micrograph of Raman sampling points for sample YT-07

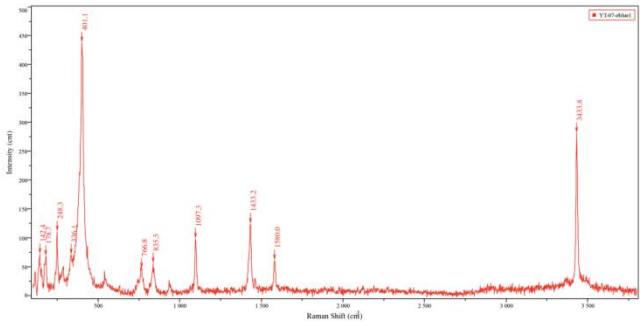

Figure 11 Raman spectrum of blue particles in sample YT-07

4.3.3 Green Pigment

The green pigment sample was designated as YT-07. Figure 12 displays the observation results of this sample under 150x magnification via a 3D video microscope, revealing evident loss of the paint layer. SEM-EDS analysis indicated that the mass fractions of Cl and Cu in YT-07 were 9.38% and 42.24% respectively. Based on these findings, the main component of the green pigment was inferred to be either atacamite/paratacamite ($Cu_2(OH)_3Cl$) or malachite ($CuCO_3 \cdot Cu(OH)_2$).

Figure 13 shows the optical micrograph of the Raman test point for sample YT-07, while Figure 14 presents the corresponding Raman spectrum. Comparison with standard spectra demonstrated that the characteristic peaks at 155.6, 177.2, 222.8, 266.7, 356.1, 431.6, 535.1, 1101.8, 1370.2, and 1498.2 cm^{-1} were consistent with the Raman characteristic peaks of malachite ($CuCO_3 \cdot Cu(OH)_2$), thus confirming the pigment's composition as malachite.

Malachite, also known as mineral green, was a rare and precious mineral pigment in ancient times. In comparison to plant-extracted greens, its color exhibits excellent long-term stability, remaining vibrant even after thousands of years. This unique property made it highly valued by painters throughout history.

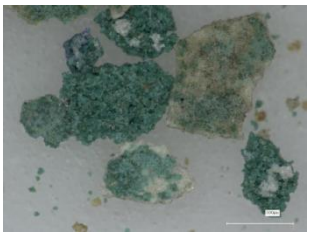

Figure 12: Three-dimensional video microscopy test results of sample YT-07

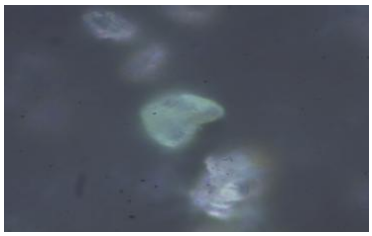

Figure 13: Optical micrograph of Raman sampling points for sample YT-07

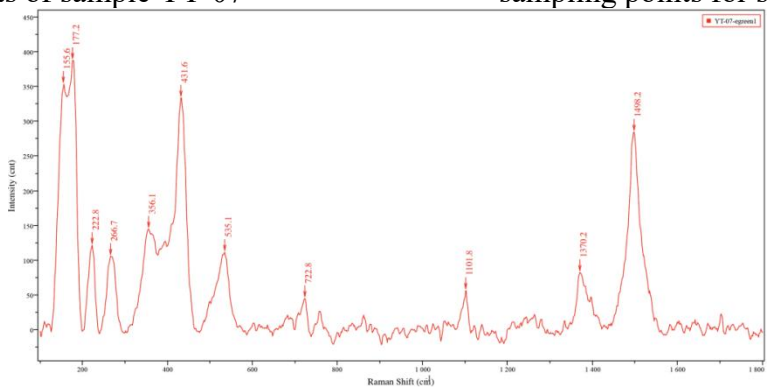

Figure 14: Raman spectrum of green particles in sample YT-07

4.3.4 Yellow Pigment

The yellow pigment sample was designated as YT-08. Figure 15 displays the microscopic image of this sample captured under 125x magnification using a 3D video microscope. Results from SEM-EDS analysis revealed a high mass fraction of Pb, reaching 90.27%, leading to the preliminary inference that the primary component of this yellow pigment is massicot or litharge (PbO).

Figure 16 presents the optical micrograph of the Raman testing point for sample YT-08, while Figure 17 shows its corresponding Raman spectrum. A comparison with standard spectra confirmed that the Raman characteristic peaks of the sample were highly consistent with the reference spectrum of PbO, thus identifying the yellow pigment as massicot (PbO).

In ancient times, massicot also had medicinal applications. Its use as a mural pigment was already prevalent during the Tang Dynasty. *Tiangong Kaiwu* (The Exploitation of the Works of Nature) documents its production process: "铅丹须文火久炼，色若秋葵" ("Minium requires prolonged refining over a gentle fire, its color resembling that of autumn sunflowers").

Figure 15: Three-dimensional video microscope test results of sample YT-08

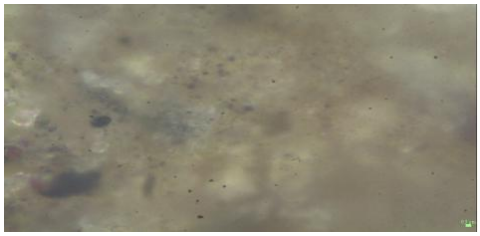

Figure 16: Optical micrograph of Raman sampling points for sample YT-08

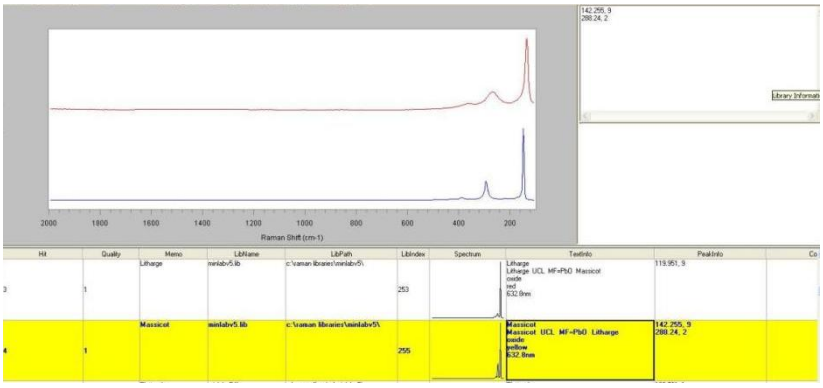

Figure 17: Raman spectrum of sample YT-08

4.3.5 White Pigment

The white pigment sample was YT-10. Figure 18 displays the micrograph of this sample under 150x magnification captured by a 3D video microscope. Figure 19 shows the optical micrograph of the Raman test point, while Figure 20 presents the Raman spectrum of sample YT-10. The Raman peaks observed at 408, 491, and 1005 cm^{-1} are in good agreement with the characteristic peaks of gypsum ($CaSO_4 \cdot 2H_2O$), thus confirming the white pigment as gypsum. Gypsum is widely used as a white pigment and is often mixed with other colorants. It is slightly soluble in water and can migrate with moisture in the mural environment, recrystallizing to exert a certain re-bonding and consolidating effect on the paint layer[2]. Most colorants can also be blended with gypsum.

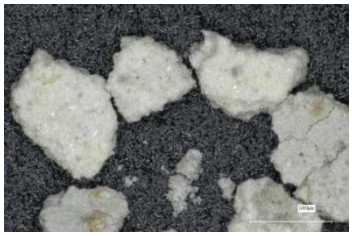

Figure 18: Sample YT-10 Three-Dimensional Video Microscope Test Result Diagram

Figure 19: Optical micrograph of Raman sampling points for sample YT-10

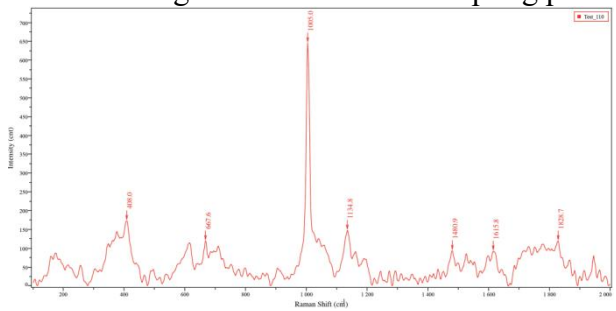

Figure 20: Raman spectrum of sample YT-10

4.3.6 Gold Foil

SEM-EDS analysis of gold foil sample YT-04 showed that the mass fractions of Au and Ag were 67.38% and 1.66% respectively, indicating relatively high purity. The detected elements Al, Si and Ca are presumed to be derived from surface contaminants. The SEM image (Figure 21) shows that the gold foil has local defects and multiple visible scratches on its surface.

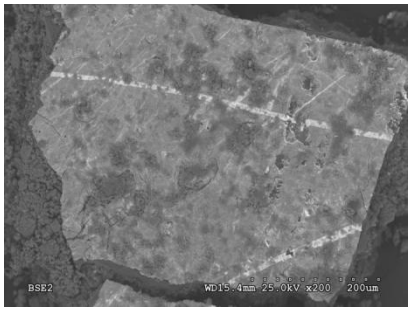

Figure 21: Scanning electron microscope image of gold foil

5. Discussion and Analysis

5.1 Production Techniques and Material System

Through microscopic cross-section analysis and on-site investigation, the plaster structure of the Yunti Temple murals is confirmed to be the typical three-layer laminated system consisting of coarse mud, fine mud and white powder. This technique differs significantly from the single coarse layer or simplified double-layer structures commonly found in contemporaneous folk temple murals in the Shanxi-Hebei-Shandong-Henan region in terms of technical complexity and finishing quality, reflecting a higher construction standard and technical requirement[3].

Laboratory analysis of the mural pigment system identified a core mineral pigment combination consisting of cinnabar, azurite, malachite, and massicot. This combination not only aligns with the material paradigm for Northern official-style polychromy recorded in Xiushi Lu ("Cinnabar substituted by cinnabar, blue derived from copper ore")[4], but also reflects pigment substitution practices in the mid-to-late Ming Dynasty based on resource availability: in the sulfur-deficient regions of North China, the more stable cinnabar was systematically chosen, replacing some natural cinnabar[5]. The use of azurite as the primary blue stands in contrast to the more frequent use of lapis lazuli in contemporary Southern temples, revealing a "local material utilization" logic in pigment selection for the Shangfangshan murals, constrained by the resources of the Taihang Mountain copper belt (e.g., Xingtai Tongye).

Overall, this mineral pigment system inherits the official Ming Dynasty tradition of "heavy color and layered dyeing" represented by murals such as those in Beijing's Fahai Temple[6]. More importantly, through the in-depth connection between "pigment source – production technique – pictorial expression," it specifically reveals the technical adaptation mechanisms that the material carriers of Ming Dynasty Buddhist art adopted to accommodate regional conditions during their secularization process[7].

5.2 Conservation and Restoration Recommendations

Based on the deterioration survey and mechanism analysis, the preservation condition of these murals is severe, with some deterioration phenomena already posing a serious threat to their structural safety and pictorial integrity. To ensure the safety of this cultural heritage, systematic conservation, restoration, and environmental control work is urgently required. Specific recommendations are as follows:

5.2.1 Implementation of Emergency Local Consolidation

For existing severe deterioration, localized intervention should be prioritized:

(1) Reattachment and Consolidation: For areas where the paint and white preparation layers have experienced large-scale flaking and cupping, appropriate adhesives should be used for penetrative reattachment and consolidation to prevent further loss.

(2) Detachment Grouting: For areas where detachment has occurred, compatible grouting materials should be used for filling and reinforcement to restore the bond between the plaster layers and the support.

(3) Crack Sealing and Compensation: Carry out necessary internal reinforcement and surface sealing for through cracks, and compensate for holes that severely affect the pictorial integrity with plaster filling and edge consolidation.

5.2.2 Control of Groundwater and Moisture Influence

The efflorescence and material loss at the bottom of the murals are primarily associated with ground moisture. Recommendations are as follows:

(1) External Drainage: Repair the drainage system around the temple to ensure rapid diversion of rainwater away from the building foundation, thereby preventing water infiltration.

(2) Internal Moisture Barrier: Where feasible, install an effective damp-proof layer on the interior floor to block the capillary rise of moisture.

5.2.3 Stabilization of the Indoor Microenvironment

To slow down the deterioration caused by drastic temperature and humidity fluctuations, recommendations are as follows:

(1) Environmental Monitoring and Control: Install temperature and humidity monitoring devices to clarify the patterns of environmental fluctuations. During rainy or high-humidity seasons, use dehumidification equipment or moisture-absorbing materials cautiously to maintain a relatively stable humidity environment.

(2) Building Maintenance: Strengthen the management of the temple’ s doors and windows, closing them promptly during rainfall to reduce the direct entry of highly humid air.

5.2.4 Establishment of Routine Maintenance and Management System

(1) Regular Dust Removal: Develop and implement a scientific periodic dust removal plan, using soft tools to gently remove surface dust so as to better reveal the colors and details of the murals.

(2) Risk Prevention and Display Management: In front of areas with severe fragmentation or extremely unstable paint layers, set up eye-catching warning signs and physical barriers to guide visitors to maintain a safe distance, preventing the aggravation of damages caused by touching or close-range breath moisture.

(3) Long-term Monitoring: Establish a system for regular inspection of deterioration and maintenance of records, tracking the development trends of key deterioration issues to provide a basis for subsequent maintenance.

In summary, from the perspectives of technique, materials, and deterioration, this study establishes a scientific record of the preservation status of the Yunti Temple murals. Its conclusions can provide key evidence for subsequent conservation and restoration practices and accumulate fundamental data for comparative studies of similar murals.

References

[1] Wang Xiongfei, Yu Lükui. *Manual for the Use of Mineral Pigments* [M]. Beijing: People's Fine Arts Publishing House, 2004.

[2] Zhou Guoxin. A Casual Talk on Ancient Chinese Pigments (Part 2) [J]. *Paint & Coatings Industry*, 1991(01):30-36.

[3] Zhang Xihuan. Traditional Chinese Pigment Minerals [J]. *China Non-Metallic Minerals Industry*, 2020,(04):10-14.

[4] Wang Yifei. A Comparison Between the Murals of Longxing Temple and Ming Dynasty Print Art [J]. New Arts, 2025,(4):183-191.

[5] Zhang Xihuan. Traditional Chinese Pigment Minerals [J]. China Non-Metallic Minerals Industry, 2020,(04):10-14.

[6] Zhang Dan. The Secular Interpretation of Mural Images in the Ming Dynasty Guanyin Temple of Xinjin, Sichuan [J]. Art Education, 2025,(11):161-164.

[7] Liu Wei. The Screen in Fresco Paintings: A Study of the 'Screen-Style Frescoes' in the Temples of Gaoping County in China[J]. Arts, 2017,6(3):13.